IJE TRANSACTIONS B: Applications Vol. 27, No. 2, (February 2014) 325-332

International Journal of Engineering

Journal Homepage: www.ije.ir

Leaching Kinetics of Stibnite in Sodium Hydroxide Solution

A. Dodangeh, M. Halali *, M. Hakim, M. R. Bakhshandeh

Department of Materials Science and Engineering, Sharif University of Technology, Tehran, Iran

PAPER INFO

Paper history:
Received 08 May 2013
Received in revised form 01 July 2013
Accepted 22 August 2013

Keywords:
Antimony Sulphide
Alkali Leaching
Dissolution Kinetics
Shrinking Core
Ash Layer

ABSTRACT

The leaching kinetics of stibnite in basic solution has been investigated. Spherical pellets of antimony sulphide were dissolved in 1 molar sodium hydroxide solutions at different temperatures. It was found that the shrinking core with ash layer model could satisfactorily explain the dissolution process. Using this model, it was found that initially the rate controlling step was a chemical reaction with activation energy of 10.2 kJ/mol. As the ash layer built up, diffusion through the ash layer became the rate controlling step. The activation energy for this step was found to be 33.4 kJ/mol. It was also observed that smaller particle size, larger solid to liquid ratio, and higher NaOH solution concentrations resulted in higher concentrations of stibnite in the leach solution.

doi: *10.5829/idosi.ije.2014.27.02b.16*

1. INTRODUCTION

Antimony is usually used as an additive in lead alloys and copper alloys. Antimony is mainly found in the form of sulphide compounds. Its most important mineral is Stibnite Sb_2S_3. Stibnite ores usually contain gold, silver, lead, and arsenic. Many researchers have concentrated on the recovery of gold from stibnite ores [1-5]. One of the major techniques for extraction of antimony has been the reduction of stibnite with iron scrap [6, 7]. The disadvantage of this technique is the dissolution of a large fraction of precious metal content in antimony. The subsequent recovery of these metals has proved impractical. Recently, new methods for treatment of antimony sulphide concentrates have been developed. These include the dissolution of antimony sulphide in an aqueous solution of hydrochloric acid saturated with chlorine [8], bio-oxidation dissolution of antimony sulphide [9], dissolution of antimony sulphide in an aqueous solution of sodium hydroxide and sodium sulphide [10], dissolution of stibnite in acid to neutral solutions [11], and dissolution of stibnite in water and hydrogen sulphide solutions [12]. Antimony can form soluble compounds in alkaline solutions. These include different forms of antimony oxy-sulphides and sulphur bearing ions. Predominance plots of various antimony species at several temperatures in reference [10] show the stability of these species at pH values larger than 7. The reactions of Sb_2S_3 in alkaline solutions are complex. These reactions, may however, be simplified as follows [2, 10].

$$Sb_2S_3 + 3\ Na_2S = 2\ Na_3SbS_3 \quad (1)$$

$$Sb_2S_3 + 2\ NaOH = NaSbOS + NaSbS_2 + H_2O \quad (2)$$

The majority of literature available on stibnite dissolution is focused on acidic solutions. There is very limited literature available on the leaching of stibnite in alkali solutions. Effect of factors such as solution ratios and degree of stirring has been studied without specifying any kinetic parameters [13]. Copper bearing ores have been leached by alkaline hypochlorite, acidic cupric chloride, and alkaline sulphide solutions to remove antimony from the ore [14]. Kinetic studies in this reference are limited to a plot of antimony recovery versus time. There are a handful of articles investigating the leaching of mechanically or chemically activated antimony bearing ores [15-18]. While these studies present valuable kinetic data including activation energies, the feed material has been mechanically activated and stibnite has not been studied in any of these references.

*Corresponding Author Email: halali@sharif.edu (M. Halali)

TABLE 1. Nomenclature used in this manuscript

Symbol	Description
t_{ch}	Time for chemically controlled process
ρ_B	Density of the solid reactant
M_B	Molar mass of solid reactant
K	Rate constant
C_A	Surface concentration of liquid reactant
N	Reaction order
r_o	Initial particle radius
r_c	Radius of the particle
gFg	Dimensionless time for chemical controlled process
X	Ratio of the initial material that has reacted
t_{DI}	time (internal diffusion controlled process)
D_g	Diffusion constant
pFg	Dimensionless time (diffusion controlled process)

Alkali leaching in the presence of sulphide ions is similar to this study. The advantage of the present work is that sulphide ions are not required. Therefore, complications such as pollution and equipment corrosion are avoided. In the present work, experimental variables which are influential on the kinetics of stibnite leaching have been studied thoroughly. These include particle size, solid to liquid ratio, solvent concentration and temperature. It has also been the aim of this study to identify and measure kinetic factors affecting the leaching of stibnite in sodium hydroxide solution. For this purpose, a high purity stibnite concentrate from "Dashkasan" antimony (gold) mine in Western Iran was used. The concentrate contained 89.1% stibnite and 10.07% silica, which formed the ash layer during the leaching process. Other constituents of the ore included 0.25% As, 0.07% Pb, 0.28% Cu, 0.14% Sodium and Potassium oxides, and traces of Sodium and Potassium sulphides. The kinetic model used was the shrinking core model. This model is consistent with experimental conditions of this research. A list of symbols used throughout this manuscript is tabulated in Table 1.

2. THEORY

The kinetic studies in this research are based on the model developed by Mazet [19]. The initial requirement for this model to be applied successfully is a sharp reaction front and the formation of an ash layer without any change in the volume of a particle. The general reaction equation is:

$$a\,(A)_l + b\,\langle B\rangle_s = c\,(C)_l + d\,\langle D\rangle_s \quad (3)$$

D is the ash layer formed and C the fluid phase produced. Since the fluid is continuously stirred, diffusion of reactants from the bulk of the fluid to the reacting particle will not be the rate controlling step. However, the reaction controlling step might be a chemical reaction at the surface of the unreacted core or the diffusion of some of the species through the ash layer. The theories associated with this model have been tabulated in Table 2. It has been the aim of this study to find the activation energy for the chemical reaction, and the diffusion rate of NaOH through the ash layer formed during the leaching of Stibnite ore. The ore was obtained from Dashkasan antimony mine, West Iran.

3. EXPERIMENTAL PROCEDURE

3. 1. Kinetic Parameter Runs High grade stibnite chunks were obtained from Dashkasan Mine. Spherical particles with radii in the range 8-8.5 mm, weighing approximately 10-11 g, with a surface area of 8-9 cm^2 were prepared manually from these chunks. The choice of the particle size was based on the largest possible spheres that could come out of the chunks. A survey of similar studies had revealed that in most cases the reaction rate had been initially dependant upon a chemical reaction [20]. With the advance of the reaction and the build up of an ash layer, the rate controlling step had become diffusion in almost all similar cases reviewed. In most cases, the critical ash layer thickness where reaction controlling step changed had been less than 1 mm. In this study, it was however decided not to take any risks and opt for a large particle size.

TABLE 2. Summary of kinetic variables for a spherical particle in the shrinking core model [19].

Mode of rate controlling step	Dependence of particle radius on time	Dimensionless time
Chemical reaction	$t_{CH}(r_c)=\frac{\rho_B}{b\,M_B\,k\,C_{A_\circ}^n}(r_\circ - r_c)$	$gFg\,(x)=1-[1-X]^{\frac{1}{Fg}}$
Diffusion through ash layer	$t_{DI}(r_c)=\frac{\rho_B}{b\,M_B\,D_g\,C_{A_\circ}}\left[\frac{r_c^3}{3r_\circ}-\frac{r_c^2}{2}+\frac{r_\circ^2}{6}\right]$	$pFg(X)=2[1-X]-3[1-X]^{\frac{2}{3}}+1$

TABLE 3. Leached stibnite (g) as a function of time and temperature

Time (s)	Temperature (K (˚C))			
	298 (25)	318 (45)	338 (65)	358 (85)
50	0.23	0.22	0.24	0.25
100	0.40	0.45	0.55	0.6
180	0.62	0.85	1.1	1.34
360	0.84	1.21	1.58	2
600	0.97	1.55	2.3	2.9
1200	1.37	2.01	2.97	3.7

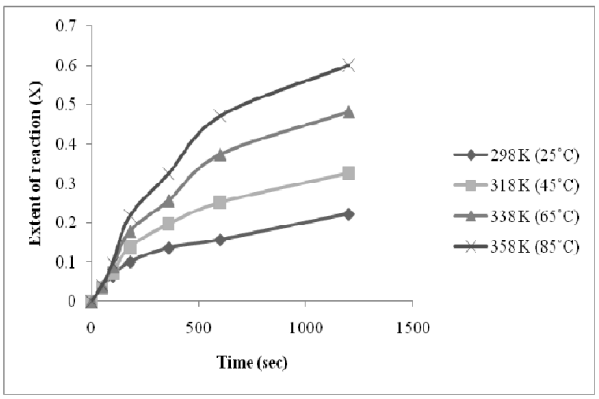

Figure 1. Effect of time and temperature on the extent of the reaction

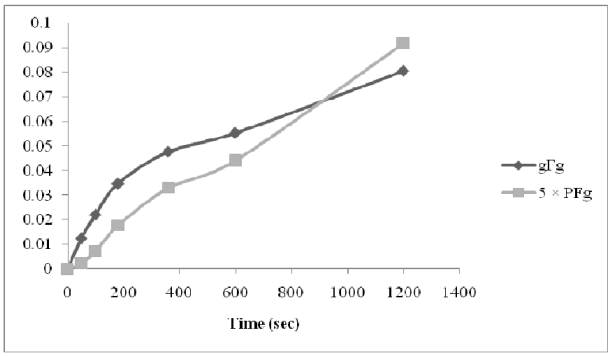

Figure 2. Variation of PFg and gFg with time at 298 K (25˚C)

Smaller particle sizes result in faster leaching rates, and therefore, higher rates of antimony production. However, activation energies of rate controlling steps do not depend on particle size. The particles were suspended from polymer threads in 500 ml sodium hydroxide solutions with a molarity of 1. Experiments were performed at temperatures of 298 K (25˚C), 318 K (45˚C), 338 K (65˚C), and 358 K (85˚C). Heating was provided by a hot plate with magnetic stirring facility. Temperature was measured constantly by a thermometer. Vigorous stirring (500 rpm) was provided by a magnetic stirrer. Samples were taken from the solutions at different time intervals and were subsequently analyzed for antimony. A glass plate was placed on the top of the container to ensure minimum loss due to evaporation from the system. Experimental results and conditions are tabulated in Table 3.

3. 2. Experimental Variable Runs These tests were conducted to find the effects of experimental variables on the leaching process. The yield in these runs is defined as $\frac{leached\ antimony}{available\ antimony}$.

3. 2. 1. Effect of Particle Size Six different particle size ranges were considered. For each test, 20 g of the sample was mixed with 1 M sodium hydroxide solution at 85˚C. The mixture was stirred at 600 rpm. The solid/liquid ratio was set to 80 g/lit. After 20 minutes, the heater was turned off. Samples were filtered and analyzed.

3. 2. 2. Effect of Solid to Liquid Ratio and Sodium Hydroxide Solution Concentration Stibnite samples were mixed with sodium hydroxide solutions at constant temperature of 85˚C. The mixtures were stirred at 600 rpm for 20 minutes. 4 sets of runs with different s/l ratios were conducted. Each set of runs was investigated under five different sodium hydroxide concentrations. Samples were filtered and analyzed.

3. 2. 3. Effect of Temperature 4 sets of experiments were conducted at different temperatures. Stibnite samples weighing 20 g were mixed with 1 M sodium hydroxide solutions. Solid to liquid ratio was set at 80 g/lit. Mixtures were stirred at 600 rpm for 20 minutes. Samples were subsequently filtered and analyzed.

4. RESULT AND DISCUSSIONS

Figure 1 shows the effect of time and temperature on the extent of the reaction (X values). The effect of time on pFg and gFg values for the runs carried out at 298 K (25˚C) are shown in Figure 2. Each plot appears to be divided into two distinct sections. Taking the gFg plot, at the time intervals smaller than 180 seconds, the diagram is almost a straight line. As the time increases, the gFg diagram loses its linearity and transforms into a curve. The pFg diagram, on the other hand, follows a reverse path. With short times, pFg is a curve. Longer times result in a linear pFg. This observation is consistent with theory. At the start of the experiment, the thickness of the ash layer is negligible; therefore, diffusion of sodium hydroxide through the ash layer is not the rate controlling stage. With increasing time, the thickness of the ash layer increases resulting in the

reaction rate control by diffusion. It is possible to calculate rate constants and the activation energy for the chemical reaction, and the diffusion constants and activation energy for diffusion of NaOH through the ash layer.

4. 1. Chemical reaction The radius of the unreacted core (r_c) may be calculated by calculating the amount of dissolved antimony. The measurements taken at the end of each run indicated that the concentration of the sodium hydroxide solution never fell below 0.97 molar. Bearing in mind that the starting concentration of the NaOH solution for each run was 1 molar, it can be assumed that the reactions are of pseudo zero order. Even if this argument is not taken into account, the concentration of NaOH solution may be assumed to be unity. It is thus possible to plot ($r_\circ$ - r_c) versus t_{CH} and obtain a straight line for the portion of the experiment where reaction rate is controlled by a chemical reaction (0 to 180 seconds). The slope of this line would be $b M_B k C_{Ao}^n / \rho_B$ according to Equation (2). Therefore, the value of the rate constant 'k' may be calculated using Equation (2) with the following substitutions:

ρ_B = 4.56 g / cm^3

M_B = 338 g / g mol

In Figure 3, ($r_\circ$ - r_c) values for all the runs are plotted versus corresponding t_{CH} values. It can be observed that the linearity is more or less retained for all runs up to an ash layer thickness of 0.03 cm. This thickness corresponds to a reaction time of 180 seconds for the 298 K (25°C) run, and 100 seconds for the 358 K (85°C) run. Calculated rate constant 'k' values are indicated in Table 4.

The activation energy for the chemical reaction may be obtained from considering the

Arhenius relation: $k = A\exp(-\Delta G/RT)$. (4)

By plotting '-ln k' values versus corresponding 1/T values a straight line with a gradient of $\Delta G/R$ is thus obtained (Figure 4). The activation energy for the chemical reaction is thus calculated as ΔG_{CH} = 10.2 kJ/mol.

4. 2. Diffusion In Figure 2 it was shown that the values of pFg plotted versus time for the 298 K (25°C) run approached a straight line in the time range > 180 seconds (corresponding to ash layer thickness larger than 0.03 cm) and it was deduced that the reaction rate is controlled by diffusion. Using Equation 3, reaction time may be plotted versus the expression $\frac{r_c^3}{3r_\circ} - \frac{r_c^2}{2} + \frac{r_\circ^2}{6}$ for all the runs (Figure 5). The slopes of the resulting straight lines are reciprocal functions of the diffusion constant. By substituting for the values of 'b', 'ρ_B', 'M_B', and '$C_{A\circ}$', the value of diffusion constant for diffusion of NaOH solution through ash layer at this temperature is calculated. Using the slopes of the straight lines and Equation 3, diffusion constants at experimental temperatures can be calculated. Results are tabulated in Table 5. By plotting -ln D values versus 1/T (Figure 6), the activation energy for the diffusion process is found to be 33.4 kJ.

TABLE 4. Rate constant values at different temperatures

Temperature (K (°C))	298 (25)	318 (45)	338 (65)	358 (85)
Rate constant × 1000 (cm/s)	1.11	1.43	1.83	2.20

TABLE 5. Diffusion constant values at different temperatures

Temperature (K (°C))	298 (25)	318 (45)	338 (65)	358 (85)
Diffusion constant × 10^5 (cm^2 / s)	1.13	2.63	6.18	10.46

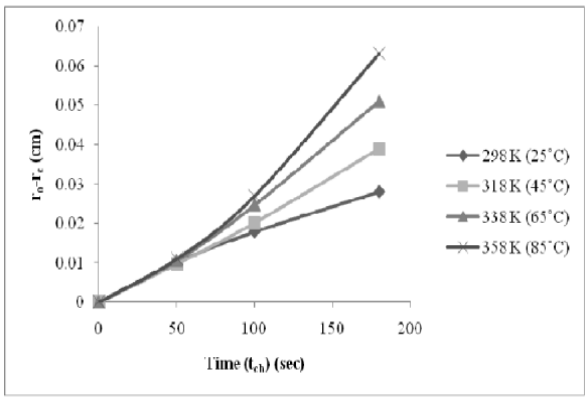

Figure 3. Variation of $r_o - r_c$ with t_{ch} for all runs

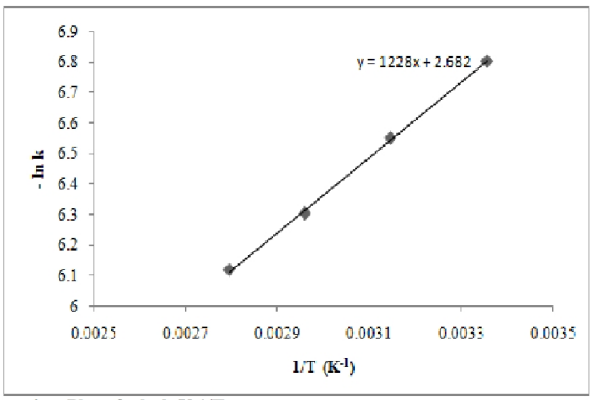

Figure 4. Plot of –ln K V 1/T

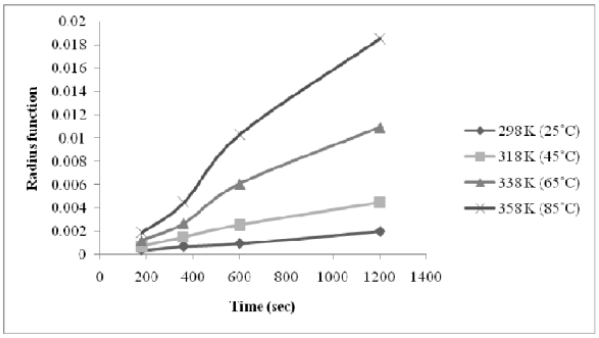

Figure 5. Variation of reaction time with radius function $(\frac{r_c^3}{3r_c} - \frac{r_c^2}{2} + \frac{r_c^3}{6})$

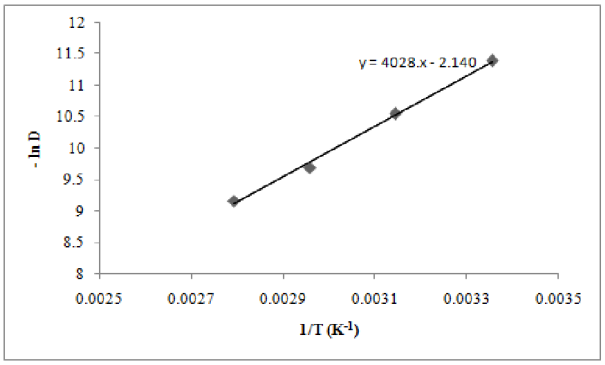

Figure 6. Plot of –ln K V 1/T

TABLE 6. Effect of particle size on the leaching of stibnite

Run No.	Particle size (mm)	Concentration of antimony (ppm)	Yield (%)
1	< 0.05	16750	32.7
2	0.05 < 0.5	16100	31.4
3	0.5 < 1	9500	18.6
4	1 < 2.8	10800	21.1
5	2.8 < 4	9300	18.2
6	4 <	4800	9.4

4. 3. Experimental Variables

4. 3. 1. Effect of Particle Size Table 6 illustrates the effect of particle size on the leaching extent at constant temperature. It is evident that reducing particle size would significantly increase leaching extent. It is not practical to reduce particle size indefinitely. Considering the results, a particle size in the range 50 – 500 µm would result in satisfactory yield values. This particle size was therefore adapted for the remainder of section 4.3 runs.

4. 3. 2. Effects of Solid to Liquid Ratio and Sodium Hydroxide Concentration Figures 7 and 8 refer to the same sets of runs. Figure 8 illustrates the effect of varying s/l ratio on leaching of stibnite with varying sodium hydroxide solution concentrations. Evidently, increasing the solid to liquid ration can enhance the amount of leaching. This observation is more prominent at higher NaOH concentrations. Increasing s/l ratio at a constant leaching concentration makes more ore available and thus the amount of leached antimony increases.

At constant s/l ratio, more leaching occurs at higher NaOH concentrations. This is evident in Figure 8. The curves in Figure 8 are not linear. Maximum yield is not attained in any of the runs either. As a matter of fact, the yield in most of the hits is around 30-35%. It is speculated that that in all cases considered, initially, leaching proceeds until the ash layer builds up to a thickness that the leaching process slows down.

4. 3. 3. Effect of Temperature Figure 9 exhibits the effect of temperature on the leaching process. As expected, the curve reveals an exponential relation between temperature and leaching extent.

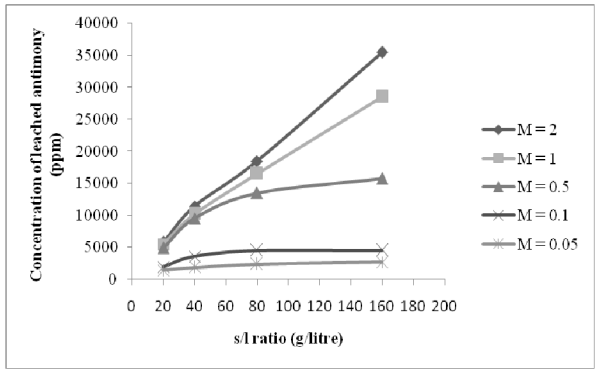

Figure 7. Effect of solid to liquid ratio on the amount of leached antimony

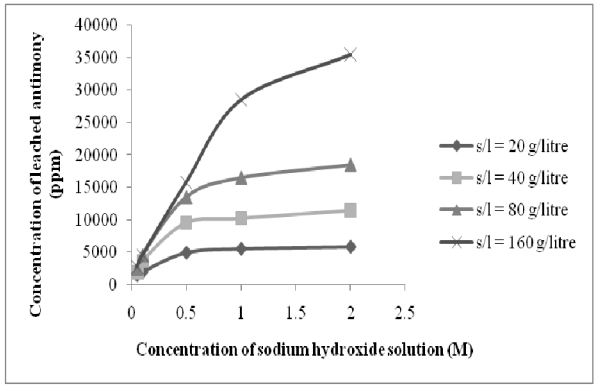

Figure 8. Effect of sodium hydroxide solution concentration on the amount of leached antimony

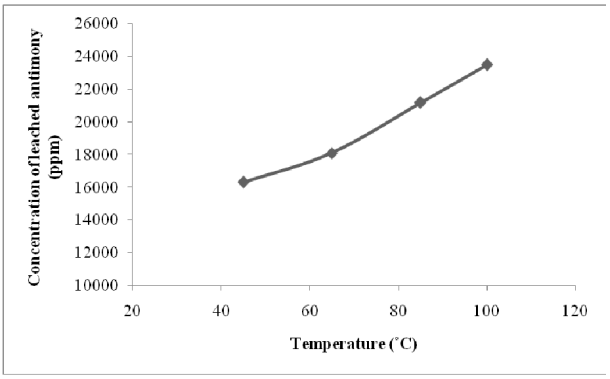

Figure 9. Effect of temperature on the amount of leached antimony

5. CONCLUSION

1. In the temperature range 298 K (25˚C) to 358 K (85˚C) the rate controlling stage in the leaching of stibnite by 1 molar solution of sodium hydroxide shifts from chemical reaction control to internal diffusion control.
2. For ash layer thickness of up to 0.03 cm, the reaction rate is controlled by a chemical reaction with activation energy of 10.2 kJ / mol.
3. For ash layer thicknesses in excess of 0.04 cm, the reaction rate is controlled by the internal diffusion of sodium hydroxide solution through the ash layer.
4. By reducing particle size and increasing solid to liquid ratio and NaOH concentration, higher antimony concentrations may be obtained.

6. REFERENCES

1. Ubaldini, S., Veglio, F., Toro, L. and Abbruzzese, C., "Combined bio-hydrometallurgical process for gold recovery from refractory stibnite", ***Minerals Engineering***, Vol. 13, No. 14, (2000), 1641-1646.
2. Ubaldini, S., Veglio, F., Fornari, P. and Abbruzzese, C., "Process flow-sheet for gold and antimony recovery from stibnite", ***Hydrometallurgy***, Vol. 57, No. 3, (2000), 187-199.
3. Brandon, N., Mahmood, M., Page, P. and Roberts, C., "The direct electrowinning of gold from dilute cyanide leach liquors", ***Hydrometallurgy***, Vol. 18, No. 3, (1987), 305-319.
4. Aghamirian, M. and Yen, W., "A study of gold anodic behavior in the presence of various ions and sulfide minerals in cyanide solution", ***Minerals Engineering***, Vol. 18, No. 1, (2005), 89-102.
5. Ubaldini, S., Fornari, P., Massidda, R. and Abbruzzese, C., "An innovative thiourea gold leaching process", ***Hydrometallurgy***, Vol. 48, No. 1, (1998), 113-124.
6. Mahlangu, T., Gudyanga, F. and Simbi, D., "Reductive leaching of stibnite (Sb_2S_3) flotation concentrate using metallic iron in a hydrochloric acid medium I: Thermodynamics", ***Hydrometallurgy***, Vol. 84, No. 3, (2006), 192-203.
7. Belzile, N., Chen, Y.-W. and Wang, Z., "Oxidation of antimony (III) by amorphous iron and manganese oxyhydroxides", ***Chemical Geology***, Vol. 174, No. 4, (2001), 379-387.
8. Çopur, M., Yartasi, A., Ozmetin, C. and Kocakerim, M., "Solubility of stibnite ore in hcl solutions saturated with Cl_2 gas", ***Chemical and Biochemical Engineering Quarterly***, Vol. 15, No. 1, (2001), 25-28.
9. Ehrlich, H., "Microbes and metals", ***Applied Microbiology and Biotechnology***, Vol. 48, No. 6, (1997), 687-692.
10. Zotov, A., Shikina, N. and Akinfiev, N., "Thermodynamic properties of the Sb (III) hydroxide complex $Sb(OH)_{3\ (aq)}$ at hydrothermal conditions", ***Geochimica et Cosmochimica Acta***, Vol. 67, No. 10, (2003), 1821-1836.
11. Shikina, N. and Zotov, A., "Solubility of stibnite (Sb2S3) in water and hydrogen sulfide solutions at temperatures of 200-300 degrees c under vapor-saturated conditions and a pressure of 500 bar", ***Geokhimiya***, Vol., No. 1, (1999), 90-94.
12. Shikina, N. D. and Zotov, A. V., "Stibnite solubility in acid to neutral solutions at 300˚c", ***Minaralogical Magazine***, Vol. 62A, , (1998), 1389-1390.
13. Emília, S. and Dagmar, R., "Investigation of the effect of some parameters on the degree of leaching antimony from stibnite", ***Acta Montanistica Slovaca***, Vol. 3,
14. Awe, S., "Selective removal of impurity elements from maurliden vastra complex sulphides flotation concentrate", ***Process Metallurgy, Luleå University of Technology, Luleå***, (2008), 42-50
15. Achimovičová, M. and Balaž, P., "Kinetics of the leaching of mechanically activated berthierite, boulangerite and franckeite", ***Physics and Chemistry of Minerals***, Vol. 35, No. 2, (2008), 95-101.
16. Baláž, P. and Achimovičová, M., "Selective leaching of antimony and arsenic from mechanically activated tetrahedrite, jamesonite and enargite", ***International Journal of Mineral Processing***, Vol. 81, No. 1, (2006), 44-50.
17. Baláž, P. and Achimovičová, M., "Mechano-chemical leaching in hydrometallurgy of complex sulphides", ***Hydrometallurgy***, Vol. 84, No. 1, (2006), 60-68.
18. Baláž, P., Achimovičová, M., Ficeriová, J., Kammel, R. and Šepelák, V., "Leaching of antimony and mercury from mechanically activated tetrahedrite $Cu_{12}Sb_4S_{13}$", ***Hydrometallurgy***, Vol. 47, No. 2, (1998), 297-307.
19. Mazet, N., "Modeling of gas-solid reaction.1. Nonporous solids", ***International Chemical Engineering***, Vol. 32, No. 2, (1992), 271-284.
20. Sokić, M., Marković, B., Matković, V., Živković, D., Štrbac, N., and Stojanović, J., "Kinetics and mechanism of sphalerite leaching by sodium nitrate in sulphuric acid solution", ***Journal of Mining and Metallurgy, Section B: Metallurgy***, Vol. 48, No. 2, (2012), 185-195.

Leaching Kinetics of Stibnite in Sodium Hydroxide Solution

A. Dodangeh, M. Halali, M. Hakim, M. R. Bakhshandeh

Department of Materials Science and Engineering, Sharif University of Technology, Tehran, Iran

P A P E R I N F O

Paper history:
Received 08 May 2013
Received in revised form 01 July 2013
Accepted 22 August 2013

Keywords:
Antimony Sulphide
Alkali Leaching
Dissolution Kinetics
Shrinking Core
Ash Layer

چکیده

در این پژوهش، سینتیک انحلال استیبنیت در محلول قلیائی بررسی شده است. نمونه‌های کروی شکل سولفید آنتیموان در محلول‌های یک مولار هیدروکسید سدیم در دماهای مختلف حل شدند. بر اساس یافته‌ها مشخص شد که انحلال این خاکه با مدل هستهٔ کوچک همراه با ایجاد لایهٔ خاکستر مطابقت دارد. همچنین مشخص شد که در آغاز واکنش، مرحلهٔ کنترل کنندهٔ نرخ یک واکنش شیمیائی با انرژی فعال سازی 10.2 kJ/mol می‌باشد. با ایجاد لایهٔ خاکستر، نفوذ از میان لایهٔ خاکستر کنترل کنندهٔ نرخ واکنش می‌شود. انرژی فعال‌سازی برای این مرحله معادل 33.4 kJ/mol می‌باشد. همچنین، ملاحظه شد که با کوچکتر شدن اندازهٔ دانه، افزایش نسبت جامد به مایع، و افزایش غلظت محلول سود می‌توان غلظت آنتیموان را در محلول حاصل از لیچ افزایش داد.

doi: *10.5829/idosi.ije.2014.27.02b.16*